ASIIMETRIK
JURNAL ILMIAH REKAYASA DAN INOVASI
p-ISSN: 2655-1861, **e-ISSN:** 2716-2923
Volume **8** Number **2**, **2026**

Effect of Low Partial Vacuum on Evaporation and Condensation Performance in a Solar Still System

Irfan Maulana Yusuf[1], Dan Mugisidi[1]*, Oktarina Heriyani[1], Sofia Pinardi[2], Nunik Pratiwi[3]
[1]Department of Mechanical Engineering, Faculty of Industrial Technology and Informatics, Universitas Muhammadiyah Prof. Dr. HAMKA, Indonesia
[2]Department of Electrical Engineering, Faculty of Industrial Technology and Informatics, Universitas Muhammadiyah Prof. Dr. Hamka, Indonesia
[3]Department of Informatics Engineering, Faculty of Industrial Technology and Informatics, Universitas Muhammadiyah Prof. Dr. Hamka, Indonesia

***Correspondence email**: *dan.mugisidi@uhamka.ac.id*

Received: 27/05/2026 Revised: 06/06/2026 Accepted: 14/06/2026

Abstract: This study investigates the effect of low partial vacuum on the evaporation and condensation performance in a solar still system. The tests were conducted using three variations: non-vacuum (101325 Pa), vacuum 1 (101313 Pa), and vacuum 2 (101309 Pa) using an exhaust system. The observed parameters included water temperature, pressure, vapor pressure difference (ΔP), evaporation mass, and condensation yield. The results showed that low partial vacuum increased the vapor pressure difference, thereby enhancing the driving force for evaporation. The highest maximum ΔP value was obtained at vacuum 2, at 1278.48 Pa. However, water temperature had a more dominant influence on total evaporation, so the highest cumulative evaporation mass was obtained under non-vacuum conditions at 8750 g due to better thermal energy retention. Meanwhile, vacuum 1 produced the highest condensation yield of 7641 g, indicating a balance between vapor formation and vapor distribution within the system. These findings suggest that the optimization of a solar still based on low partial vacuum is determined not only by an increase in vapor pressure difference but also by the system's ability to retain thermal energy and the effectiveness of the condensation process.

Keywords: vacuum; desalination; evaporation; condensation; still

6 CLEAN WATER AND SANITATION

SDGs Problem Solving

This research contributes to SDGs Chapter #6 by improving the efficiency of seawater desalination using partial vacuum in solar stills, facilitating sustainable freshwater production with renewable energy, and providing solutions to water scarcity, particularly in coastal and remote regions that lack access to clean water supply.

Conflict of Interest Statement: The author(s) declares that the research was conducted in the absence of any commercial or financial relationship that could be construed as a potential conflict of interest.

Jurnal Asiimetrik: Jurnal Ilmiah Rekayasa dan Inovasi - ASIIMETRIK is an open access and peer-reviewed journal published by Faculty of Engineering, Universitas Pancasila, Indonesia.

1. INTRODUCTION

The demand for clean water continues to rise alongside population growth, industrial activity, and climate change, which affect the availability of clean water sources (Gaur *et al.*, 2021). Water is a vital resource for life; approximately 97% of it is saltwater in the oceans, while the remaining 3% is freshwater found in groundwater, lakes, and rivers (Dina *et al.*, 2017). One technology that has been extensively developed to address this issue is desalination (Yusuf *et al.*, 2023). Desalination offers a potential solution for converting seawater into freshwater (Munawar *et al.*, 2022). The desalination process involves two stages: evaporation and condensation, facilitated by thermal energy in a vacuum system or via a heater plate (Yan *et al.*, 2021). One simple method used in Indonesia is desalination that relies on solar energy as the primary heat source, known as a solar still (Lubis and Munawar, 2019). Solar energy was chosen due to its unlimited availability, given that desalination equipment requires high-temperature energy and sufficient intensity (Andrés-Mañas *et al.*, 2020). However, the performance of solar stills remains relatively low, particularly regarding evaporation rate and distilled water production. Various efforts have been made to improve system performance, including design modifications, heat absorption, and optimization of operating conditions (Tarif *et al.*, 2025). Therefore, a more effective method to enhance the evaporation process is required, one of which is the application of partial vacuum pressure.

The use of a vacuum in desalination aims to accelerate evaporation (Agustina, Sudarti and Yushardi, 2020). A vacuum environment accelerates the evaporation process (Al-Obaidi *et al.*, 2025). The application of vacuum in this system is an innovative step that marks a significant departure from conventional methods (Tanusekar and Sutanhaji, 2014). Theoretically, reducing the pressure within the system can increase the vapor pressure difference between the water surface inside the system and the air above it.

Although previous studies have shown that the application of vacuum can enhance the evaporation process in desalination systems, most studies still rely on active vacuum pumps operating at relatively high vacuum levels, which require significant energy consumption (Susanto *et al.*, 2024). Research utilizing low-cost exhaust-based systems to generate partial vacuum under conditions close to atmospheric pressure remains limited, particularly in salt pond-scale solar still systems (Gkountas *et al.*, 2022). Furthermore, most studies focus on increasing the evaporation rate without comprehensively evaluating the relationship between pressure drop, water temperature, vapor pressure difference, and condensation yield (Ambarita, 2018; Ayoobi and Ramezanizadeh, 2022). Therefore, further research is needed to understand how low partial vacuum conditions affect both evaporation and condensation performance simultaneously under simpler and more energy-efficient operating conditions.

In a solar still, evaporation performance is influenced not only by the temperature of the water as a source of thermal energy, but also by the vapor pressure distribution within the evaporation chamber (Alamsyach *et al.*, 2024). A decrease in partial pressure has the potential to increase the vapor pressure gradient, thereby increasing the driving force for mass transfer (Haji, Wirosoedarmo and Tyas, 2018). However, this condition can also affect vapor distribution and condensation mechanisms, especially when the airflow within the chamber becomes too high.

Therefore, experimental studies are needed to understand the interaction between temperature, partial pressure, and vapor transport mechanisms in solar still systems. This study aims to analyze the effect of low partial vacuum generated using exhaust on the evaporation and condensation performance of seawater in a solar still system. The novelty of this study lies not only in the application of an exhaust-based low partial vacuum system to a salt pond-scale solar still, but also in the evaluation of the interaction between vapor pressure differences, water temperature, evaporation rate, and condensation yield under low vacuum conditions. This study provides an understanding of the role of low partial vacuum in mass transfer mechanisms and vapor distribution, which has rarely been discussed in previous research on solar still systems. The contribution of this study is to provide an experimental basis regarding the effect of low partial vacuum on evaporation and condensation performance in solar still systems, thereby serving as a more cost-effective alternative compared to vacuum pump-based systems.

2. METHODOLOGY

This study is an experimental investigation designed to analyze the effect of applying a vacuum on the evaporation rate of seawater in a solar still system, using three system configurations: non-vacuum, one exhaust (vacuum 1), and two exhausts (vacuum 2), with the aim of controlling pressure changes within the salt pond chamber. Under conditions without exhaust, with pressure approaching atmospheric pressure (101325 Pa), the system is in a closed state, so that the mass transfer of water vapor occurs through natural diffusion (Oktavian *et al.*, 2024). Meanwhile, in the Vacuum 1 (101313 Pa) and Vacuum 2 (101309 Pa) variations, forced air circulation occurs, causing a decrease in partial pressure within the chamber, thereby creating a vacuum condition (Sayuti *et al.*, 2023). Pressure is one of the primary factors influencing the evaporation process.

Data collection was conducted for 9 hours per day, from 8:00 am to 5:00 pm WIB, over a period of 3 days for each test variation. Data on temperature, pressure, and other parameters were recorded at 15-minute intervals throughout the testing period. The tests were conducted under natural weather conditions, with solar radiation intensity monitored throughout the experiment.

Data obtained were calculated as mean values. The distribution of the measurement data was analyzed using standard deviation to determine the level of data consistency during the testing. The standard deviation was calculated using the following equation (Dwibowo *et al.*, 2025):

$$s = \sqrt{\frac{\sum_{i=1}^{n}(x_i - \bar{x})^2}{n-1}} \tag{1}$$

where s is the standard deviation, x_i is the measured data, $\bar{x}$ is the mean, and n is the number of test data points. The instruments and specifications listed in Table 1 were used to perform measurements and collect data in this study.

Before testing began, all measuring instruments were inspected and verified in accordance with the manufacturer's specifications to ensure they were functioning properly. Measurements of temperature, pressure, and solar radiation intensity were taken using factory-calibrated instruments and within their recommended measurement ranges. A preliminary check was conducted by comparing the readings with actual environmental conditions before experimental data collection began.

Table 1. Measurement tools

No	Tool	Function	Specification
1	Digital Thermometer	Measuring temperature (T1-T3)	-50 ℃-110 ℃, ± 0.1 ℃
2	Digital Hygrometer	Measuring relative humidity (RH1-RH3)	10%-99%, ± 1%
3	Pressure Meter PCE-PDA	Measuring pressure	Range -20 ÷ 20 Pa
4	Solar Meter	Measuring solar radiation intensity	1-3999 W/m^2
5	Vernier Caliper	Measuring water level	Scale 0.05 mm
6	Digital Scale	Measuring condensation yield	0-5 kg, 1 g

The salt pond is designed with dimensions of 7000 mm in length, 1500 mm in width, and 1100 mm in height. The pond cover features a sloped surface designed to optimize solar radiation absorption and to direct condensate water flow toward the collection tank. The pool cover uses transparent plastic placed inside the frame, while the base structure is made of 8 mm thick plywood and the basin walls use 12 mm thick wooden boards (Figure 1). The pool bottom is lined with a geomembrane that functions as a waterproof layer capable of absorbing radiation, as well as facilitating salt precipitation (Sayuti *et al.*, 2023). The material, function and specification of research instrument design and sensor positions shown in Table 2.

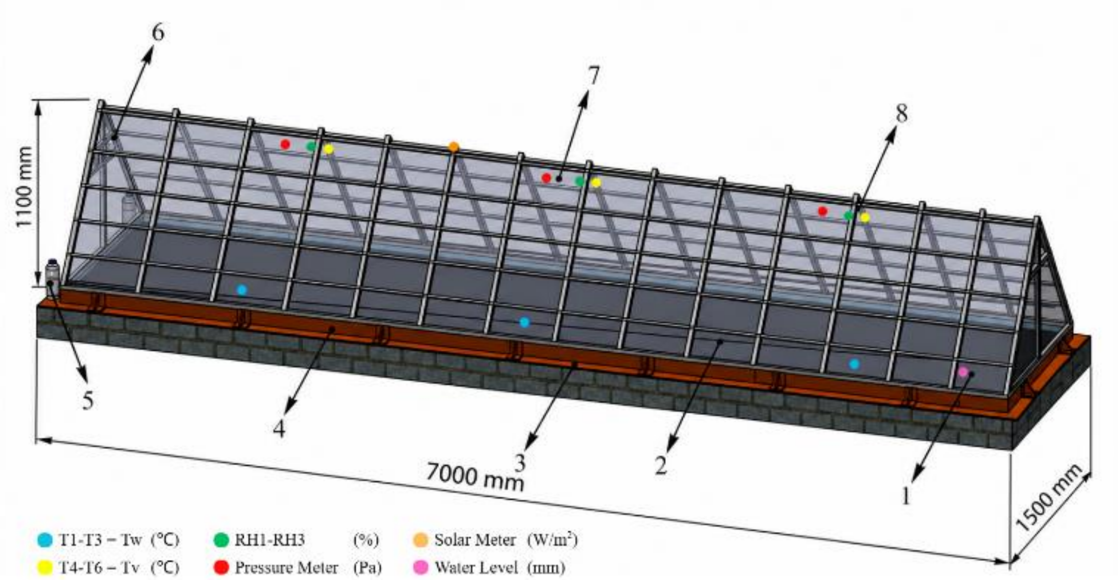

Figure 1. Research instrument design and sensor positions

This study was conducted in the courtyard of the Mechanical Engineering Laboratory, Faculty of Industrial Technology and Informatics, Prof. Dr. HAMKA Muhammadiyah University in January 2026, with an initial test volume of 420 liters of seawater. The apparatus used in this study is illustrated in the schematic diagram shown in Figure 2.

The pressure reduction in this study falls under the category of low partial vacuum, with a relatively small pressure difference compared to atmospheric pressure. Nevertheless, the change in pressure still affects the partial pressure of water vapor within the enclosed space, thereby increasing the evaporative mass transfer gradient. These conditions allow for an increase in the evaporation rate during the early stages of the test, particularly as the water temperature begins to rise.

Table 2. Materials

No	Material	Function	Specification
1	Geomembrane HDPE	Lining the basin base and preventing water leakage	Thickness 500 micron (0.5 mm), 7 m x 1.5 m
2	Water Gutter	Channeling condensed water to the collection bottle	PVC pipe 1”
3	Wood Board	Basin wall structure	Thickness 12 mm, length 1200 mm, height 90 mm
4	Plywood	Basin base	Thickness 8 mm
5	Freshwater Container	Collecting condensed water	1.5 L bottle
6	Exhaust Fan	Generating partial vacuum to enhance evaporation	2 units, 4” diameter, airflow rate 180 m^3/h, 2800 rpm
7	UV Plastic	Covering the chamber and preventing vapor loss	Transparent, transmissivity (τ) 0.90, thickness 50 micron
8	Frame Structure	Main supporting structure	30 x 30 mm, light steel

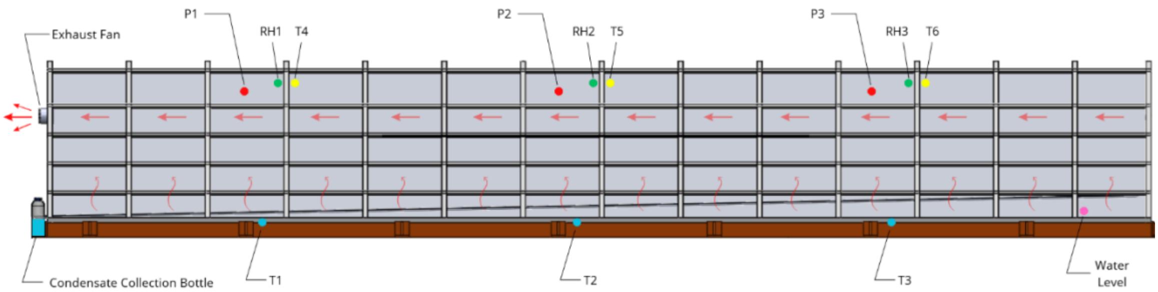

(a). Side view

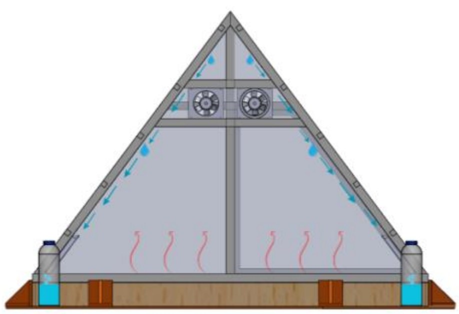

(b). Font view

Figure 2. Schematic research instrument

The pressure measured during testing is gauge pressure, which is pressure relative to atmospheric pressure. Absolute pressure is not measured directly but is calculated using atmospheric pressure as a reference value. The relationship between absolute pressure and gauge pressure is expressed in Equation (2), where absolute pressure is obtained by adding atmospheric pressure to gauge pressure. Using this method, relatively small changes in pressure relative to atmospheric pressure can still be analyzed to determine their effect on the evaporation and condensation processes within the solar still.

$$P_{abs} = P_{atm} + P_g \quad (2)$$

where (P_{abs}) is the absolute pressure (Pa), (P_{atm}) is the atmospheric pressure (Pa) dan (P_g) is the gauge pressure (Pa).

The exhaust system was used to create a low partial vacuum by drawing air out of the evaporation chamber into the surrounding environment. The resulting pressure drop causes the partial pressure of air inside the chamber to decrease, thereby increasing the vapor pressure difference between the water surface and the air above it. In addition to reducing pressure, the airflow generated by the exhaust system can also affect the distribution of water vapor within the evaporation chamber and may carry some of the vapor out of the system during the testing process.

During the test, the drop in water level (L) was observed periodically and used to determine the amount of water that evaporated. The volume of evaporation was calculated by multiplying the change in water level by the area of the salt pond, as expressed (Dwibowo *et al.*, 2025):

$$V = \Delta h \times A \quad (3)$$

where V is the volume of water that evaporates (g/day), Δh is the decrease in water level (mm), and A is the surface area of the salt pond (m²). Since the salt pond is rectangular, the surface area is calculated equation (4).

$$A = p \times l \quad (4)$$

where p is the length of the salt pond (m) and l is the width of the salt pond (m).

Figure 3 illustrates the process of collecting data on evaporation and determining the condensation results. Solar radiation penetrates the transparent plastic cover and is absorbed by the black pool bottom (geomembrane), which has an absorption coefficient of 0.98 (Hoiriyah, 2021).

Figure 3. Solar still desalination process

The absorbed heat is then transferred to the seawater, thereby increasing its temperature. This temperature increase causes the saturated vapor pressure of the water to rise, driving evaporation (Shareef, Kurji and Hamzah, 2024). The resulting water vapor fills the space inside, while the salt remains behind and settles at the bottom. Water vapor adhering to the surface of the cover condenses, forming water droplets on the inner side of the cover (Elazab, Elshaarawy and Dahab, 2026). The droplets flow down the slope of the cover toward the freshwater collection bottle.

3. RESULTS AND DISCUSSION

In a closed solar still system, the evaporation process is influenced by the interaction between water temperature and pressure conditions within the chamber (Sachidananda *et al.*, 2025). A decrease in partial pressure due to the use of an exhaust system has the potential to increase the vapor pressure gradient between the water surface and the surrounding air, which serves as the primary driving force in the mass transfer process (Dwibowo *et al.*, 2025). However, the contribution of the pressure parameter must be analyzed in conjunction with temperature, as both influence each other in determining the amount of vapor formed and distributed within the system. The system's effectiveness is highly dependent on the evaporation rate. The higher the evaporation rate, the greater the system's thermal efficiency, as heat energy is directly absorbed to convert water into vapor (Mugisidi *et al.*, 2021).

(a). Two fan (b). One fan (c). No fan

Figure 4. Exhaust fan variations

Variations in these factors (Figure 4) directly influence the vapor pressure conditions and the mechanisms of water vapor transport within the system, which ultimately affect the processes of evaporation and condensation (Feria-Díaz *et al.*, 2022). The initial stage of the experiment is represented by the solar radiation intensity graph, which shows an increasing trend from morning to midday, followed by a gradual decrease in the afternoon.

Figure 5 shows that this pattern aligns with changes in the sun's position, which affect the amount of radiant energy received by the surface of the salt pond. The highest radiation intensity was recorded in the non-vacuum variation (101325 Pa), ranging from approximately 600 to 700 W/m². These conditions indicate that the thermal energy received by the system in the non-vacuum variation is relatively greater than in the other variations. The radiant energy absorbed by the geomembrane layer at the bottom of the basin is then converted into thermal energy and transferred to the seawater through conduction and convection mechanisms, causing the water temperature to rise gradually in accordance with the pattern of changes in solar radiation (Oktavian *et al.*, 2024).

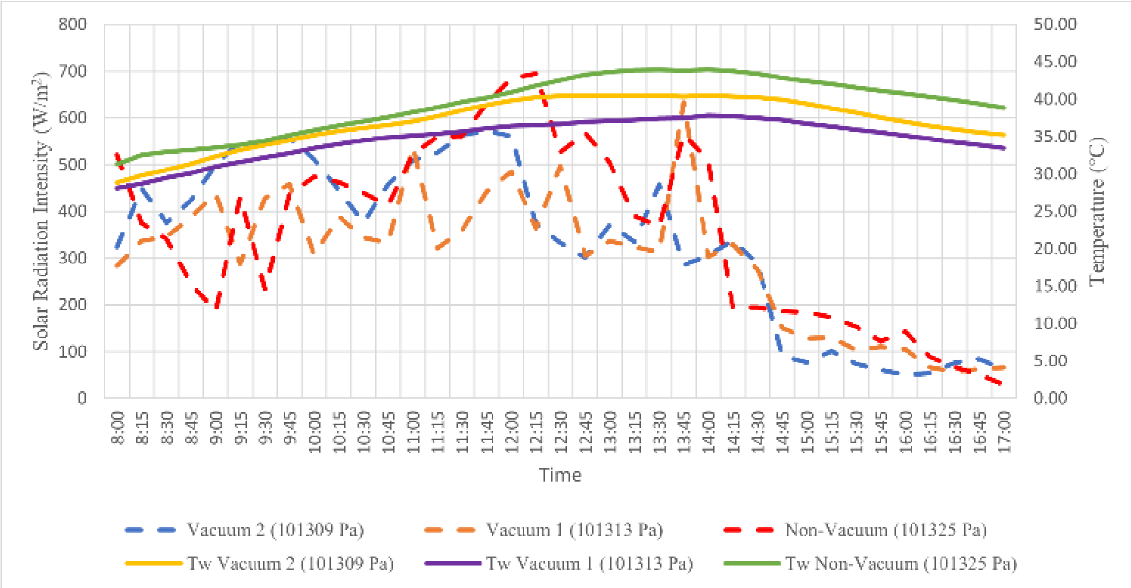

Figure 5. Solar radiation intensity and water temperature

The rise in temperature indicates that the heat energy absorbed by the system exceeds the heat loss occurring through convection, radiation, and evaporation (Mugisidi *et al.*, 2023). This temperature increase directly affects the rise in the saturated vapor pressure of water. Thermodynamically, as the temperature increases, the kinetic energy of water molecules increases, making it easier for molecules to transition from the liquid phase to the vapor phase (Ambarita, 2018). Consequently, the rate of water vapor formation at the surface increases. This phenomenon demonstrates that water temperature acts as one of the primary factors controlling evaporation potential in a solar still system.

Under non-vacuum conditions, the temperature reached a maximum of 43.95 °C because the system was closed with no outflow of air, causing more thermal energy to accumulate within the evaporation chamber. This condition resulted in reduced heat loss due to air circulation and enhanced the system’s ability to retain thermal energy (Sayuti *et al.*, 2023). Conversely, under partial vacuum conditions, the use of an exhaust creates air circulation that accelerates the release of latent heat along with the water vapor flow, causing some thermal energy to exit the system (Dwibowo *et al.*, 2025). Consequently, the water temperature under vacuum conditions tends to be lower compared to non-vacuum conditions.

Although a partial vacuum has the potential to increase the driving force of evaporation by increasing the vapor pressure difference, research results indicate that temperature has a more dominant influence on the accumulation of total evaporation mass (Al-Obaidi *et al.*, 2025). This is evident in the non-vacuum conditions, which produce the highest temperature and consequently yield the largest cumulative evaporation mass. This phenomenon indicates that increased evaporation in a solar still system is not only determined by pressure conditions but is also significantly influenced by thermal energy during the process (Yan *et al.*, 2021).

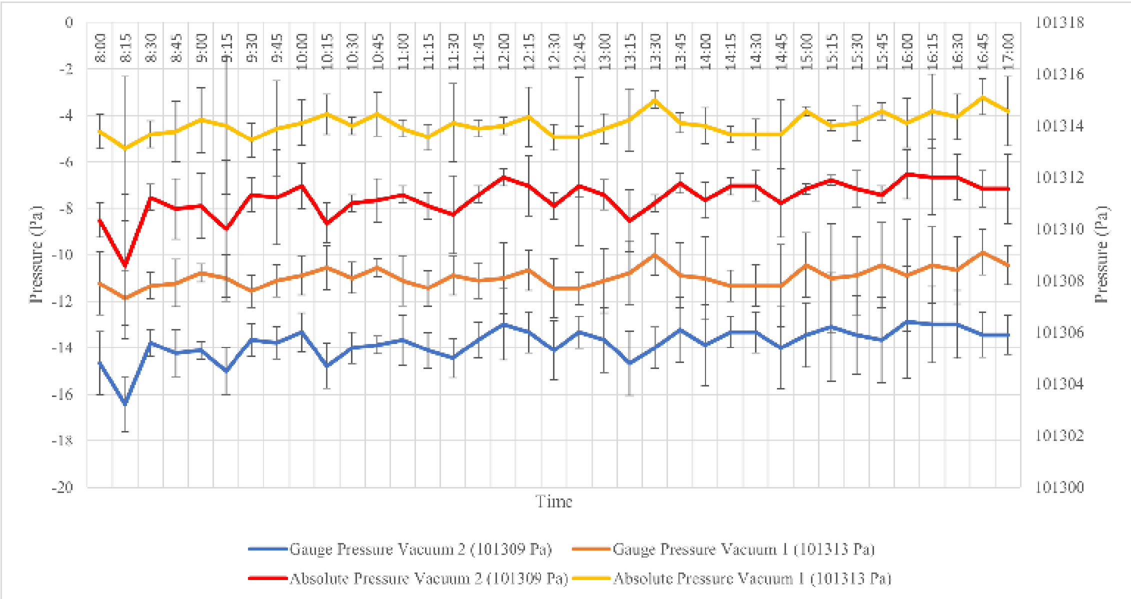

Figure 6. Gauge and absolute pressure vacuum 2 (101309 Pa) and vacuum 1 (101313 Pa)

The absolute pressure values shown on the graph are obtained by converting gauge pressure using atmospheric pressure as a reference value. Figure 6 shows the variations in gauge pressure and absolute pressure under vacuum conditions 1 and 2 during the experimental process. In general, the absolute pressure in both variations tended to be stable with relatively small fluctuations throughout the observation period, while the gauge pressure showed negative values indicating the formation of sub-atmospheric pressure conditions. These conditions indicate that the system successfully generated a partial vacuum by an exhaust during the evaporation process (Yusuf *et al.*, 2023).

Vacuum 2 produces a lower absolute pressure and a more negative gauge pressure compared to Vacuum 1. This indicates that using two exhausts creates a greater suction effect, resulting in a more significant drop in air pressure within the evaporation chamber. This pressure drop causes a reduction in the partial pressure of water vapor in the evaporation chamber and, theoretically, can increase the vapor pressure gradient between the water surface and the surrounding air. The greater the vapor pressure gradient formed, the greater the driving force for mass transfer, which has the potential to accelerate the evaporation process (Dwibowo *et al.*, 2025).

Nevertheless, the measurement results indicate that the pressure reduction achieved in this study still falls within the category of low partial vacuum, with a relatively small pressure difference compared to atmospheric pressure (Susanto *et al.*, 2024). This is evident from the absolute pressure, which remains in the range of 101309-101314 Pa. Thus, although there is an increase in the driving force of evaporation due to the pressure drop, its contribution to the increase in total evaporation is likely not yet fully dominant compared to the influence of water temperature as the primary energy source for phase change.

In addition, pressure fluctuations occurring during testing can be influenced by changes in solar radiation intensity, temperature increases, water vapor formation, and variations in airflow due to exhaust operation. As the temperature rises, the amount of vapor formed also increases, causing the pressure conditions inside the chamber to change dynamically (Alamsyach *et al.*, 2024).

However, the error bars, as indicated by the relatively small standard deviation, suggest that the system can maintain pressure stability throughout the testing process. The low standard deviation also indicates that the measurement results exhibit good repeatability, meaning that operating conditions under each variation can be considered consistent.

Overall, the pressure measurement results indicate that the system was able to maintain a stable low partial vacuum throughout the testing process. Vacuum 2 produced a lower pressure than Vacuum 1, thereby potentially increasing the mass transfer driving force (Wirangga *et al.*, 2023). The vapor pressure difference is a key parameter determining the mass transfer driving force during the evaporation process (Mugisidi *et al.*, 2021):

$$\Delta P = P_w - P_v \tag{5}$$

The greater the ΔP value, the greater the potential for vapor mass transfer from the water surface to the air space above it (Dwibowo *et al.*, 2025). In this study, the use of an exhaust caused a decrease in the partial pressure of the air, resulting in a lower vapor pressure. This condition increased the ΔP value and accelerated the evaporation process in the early stages of the test. However, the increase in ΔP did not directly result in the highest cumulative evaporation mass, as vapor formation remains heavily influenced by temperature as the primary energy source for evaporation.

$$P_w = exp\left[25.317 - \left(\frac{5144}{T_w + 273}\right)\right] \tag{6}$$

$$P_v = exp\left[25.317 - \left(\frac{5144}{T_v + 273}\right)\right] \tag{7}$$

where P_w is the saturated vapor pressure of water, T_w is the water temperature, P_v is the vapor pressure of air, T_v is the indoor air temperature.

The decrease in absolute pressure observed in this study was relatively small compared to atmospheric pressure. In vacuum 1, the pressure dropped to 101313 Pa, or approximately 0.0118%, while in vacuum 2, it dropped to 101309 Pa, or approximately 0.0158%. These values indicate that the conditions created constituted a low partial vacuum. Physically, a pressure drop of a few Pascals is not yet dominant enough to control total evaporation. However, this pressure change can still reduce the partial pressure of air within the evaporation chamber, thereby increasing the vapor pressure difference, especially in the early stages of the test.

The increase in vapor pressure difference in this study was not only caused by the pressure drop due to exhaust but was also significantly influenced by the rise in water temperature. Higher water temperatures increase the saturated vapor pressure of water, thereby increasing the ΔP value. Therefore, although Vacuum 2 produced the greatest pressure drop and the highest ΔP, the largest cumulative evaporation mass was still obtained under non-vacuum conditions because the water temperature and available thermal energy were higher.

The ΔP value is obtained from the difference between the saturated vapor pressure of water at the liquid surface and the vapor pressure of air within the evaporation chamber. The higher the ΔP value, the greater the tendency of water molecules to transition from the liquid phase to the vapor phase

(Yan *et al.*, 2021). Thus, an increase in ΔP will theoretically increase the potential evaporation rate in a solar still system.

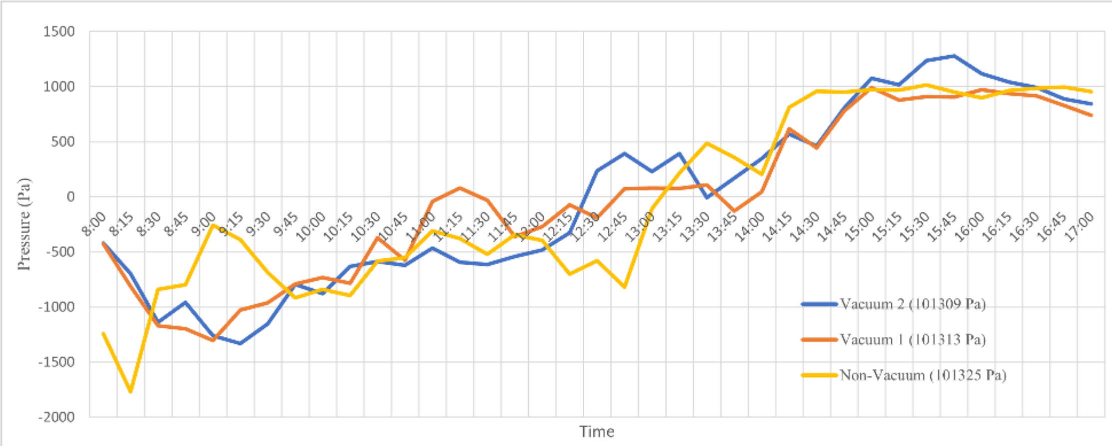

Figure 7. Vapor pressure difference (ΔP)

In this study, the use of an exhaust caused a decrease in the partial pressure of air inside the chamber, resulting in a lower air vapor pressure. This condition increased the ΔP value and produced a greater driving force for mass transfer compared to conditions without a vacuum. The test results in Figure 7 show that the highest maximum ΔP value was obtained at vacuum level 2 at 1278.48 Pa, followed by vacuum level 1 at 1016.60 Pa, and non-vacuum at 991.55 Pa. These results indicate that increasing the exhaust volume can enhance the reduction in partial pressure and consequently increase the vapor pressure gradient within the system.

At the start of the test, the ΔP value tends to be low because the temperature is still relatively low, so the saturated vapor pressure formed at the water's surface has not yet increased significantly. As the test time increases and the temperature rises due to the absorption of solar radiation energy, the saturated vapor pressure of water increases, causing ΔP to rise gradually until it reaches a maximum value. This phenomenon indicates that the change in ΔP is not only influenced by the decrease in partial pressure due to the vacuum but is also influenced by the increase in temperature, which determines the magnitude of the saturated vapor pressure (Susanto *et al.*, 2024).

Although vacuum variation 2 produced the highest ΔP value, this condition did not directly result in the largest cumulative evaporation mass. The research results show that the highest evaporation mass was obtained under non-vacuum conditions. This phenomenon indicates that an increase in the mass transfer driving force due to a larger ΔP does not necessarily result in an increase in total evaporation if the thermal energy available for the phase change process remains limited. In other words, evaporation in a solar still system is the result of the interaction between the mass transfer driving force due to ΔP and the availability of thermal energy to support vapor formation (Dwibowo *et al.*, 2025).

In addition, an excessively high vacuum can potentially accelerate the movement of water vapor within the chamber, thereby shortening the vapor's residence time. This condition can result in some of the vapor not undergoing optimal condensation or even being carried out with the airflow (Sayuti *et al.*, 2023). Therefore, an increase in ΔP must be balanced with appropriate thermal conditions and flow distribution to ensure that the evaporation and condensation processes occur more effectively.

The pressure reduction observed in this study is still relatively low compared to atmospheric pressure. Nevertheless, this low partial vacuum condition still causes a decrease in the partial vapor pressure within the evaporation chamber, thereby increasing the vapor pressure difference. The results of the study indicate that even this relatively small change in pressure is still capable of influencing evaporation and condensation characteristics, particularly during the early stages of the evaporation process.

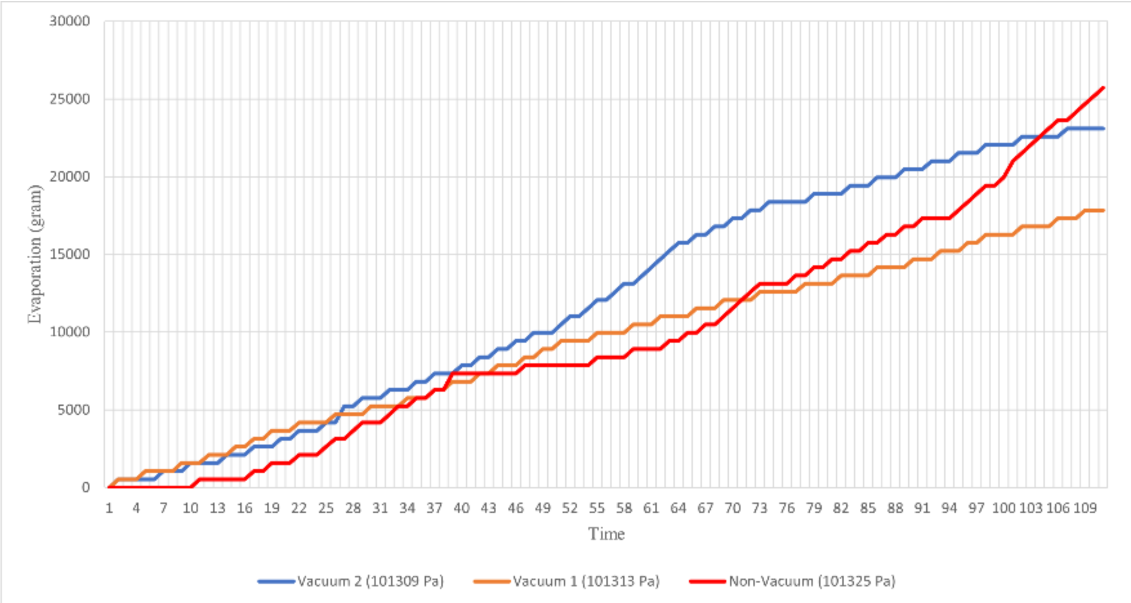

Figure 8. Evaporation rate

Figure 8 shows that, under vacuum condition 2, the evaporation rate tended to be higher during certain test periods compared to vacuum condition 1 and the non-vacuum condition. This phenomenon aligns with the ΔP measurement results, which indicate that vacuum 2 produces the highest vapor pressure difference. This suggests that an increase in exhaust volume contributes to a decrease in partial pressure, causing the evaporation process in the initial stage to proceed more intensively (Dwibowo *et al.*, 2025). In other words, a low partial vacuum enhances evaporation potential by increasing the driving force for mass transfer.

Although a low partial vacuum can increase the vapor pressure difference and the driving force for mass transfer, these increases do not directly result in higher evaporation rates or maximum condensation yields. In this study, the decrease in absolute pressure was only 0.0118% at vacuum 1 and 0.0158% at vacuum 2 relative to atmospheric pressure. These values indicate that the effect of low partial vacuum acts more as a supporting factor that enhances evaporation potential, while the availability of thermal energy becomes the main factor controlling vapor generation during the test. However, in the final stage of the test, the non-vacuum condition resulted in a higher evaporation rate. This phenomenon indicates that the effect of water temperature on vapor formation is more dominant than the effect of a low partial pressure reduction (Yusuf *et al.*, 2023). Under non-vacuum conditions, heat energy tends to accumulate more within the chamber due to minimal heat loss through outgoing airflow. These conditions cause the temperature to rise, thereby increasing the conversion of the liquid phase into vapor (Susanto *et al.*, 2024).

These results indicate that the increase in evaporation rate in a solar still system is influenced not only by the magnitude of ΔP but also by the accumulation of thermal energy (Alamsyach *et al.*, 2024). Although a partial vacuum enhances the driving force for evaporation, heat loss due to air circulation can lower the temperature and reduce the energy available for phase change (Pratama, Mugisidi and Heriyani, 2026). Therefore, there is an interaction between thermodynamic and mass transfer factors that collectively determine evaporation performance. Additionally, the use of an exhaust with a larger capacity has the potential to cause the airflow within the chamber to become too rapid, resulting in some thermal energy being carried out along with the water vapor. This condition can lead to a decrease in the efficiency of thermal energy utilization within the system. This phenomenon explains why an increase in vacuum level does not always result in the highest cumulative evaporation in this study.

Thus, optimizing the performance of a solar still requires more than simply increasing the vacuum level; it is also necessary to consider the balance between increasing the driving force for evaporation (Yusuf *et al.*, 2023). Consequently, the combination of thermal conditions and partial pressure is a key factor in determining overall evaporation performance.

These results are consistent with a study by Mugisidi et al., that showing increasing the vacuum can enhance the driving force of evaporation (Mugisidi *et al.*, 2021). However, in this study, temperature was found to be a more dominant factor than a reduction in low partial pressure. Therefore, increasing the low partial pressure using a simple exhaust system has the potential to serve as an alternative for enhancing evaporation, though its effectiveness remains dependent on thermal energy.

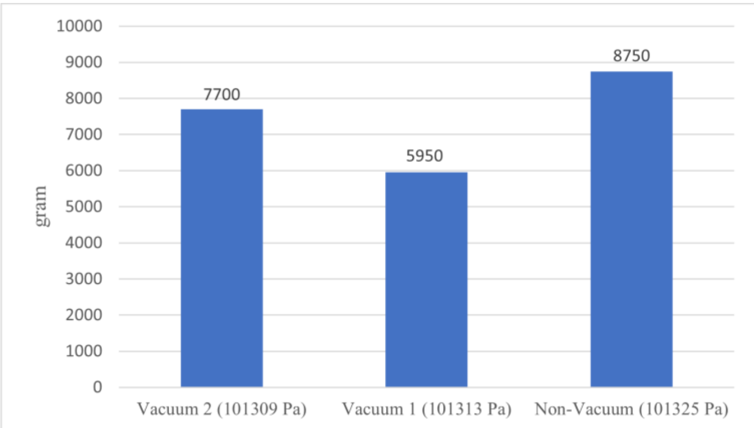

Figure 9. Cumulative evaporation mass

The effect of temperature and pressure on the evaporation process is clearer in Figure 9, which shows the cumulative evaporation mass during the test. The results show that the highest evaporation mass was obtained under non-vacuum conditions (101325 Pa) at 8750 grams, followed by vacuum 2 (101309 Pa) at 7700 grams and vacuum 1 (101313 Pa) at 5950 grams. These results indicate that although vacuum 2 produced the highest ΔP value and a greater driving force for evaporation, this condition did not result in the largest cumulative evaporation mass (Sayuti et al., 2023). Under non-vacuum conditions, the evaporation chamber is in a more sealed state, resulting in reduced heat loss due to air circulation. This condition allows thermal energy to accumulate more effectively within the system and produces higher temperatures during the test (Yusuf *et al.*, 2023).

The results of the study show that increasing the vacuum level from vacuum 1 to vacuum 2 results in an increase in cumulative evaporation mass. This indicates that an increase in partial vacuum continues to contribute to increased evaporation (Curto, Franzitta and Guercio, 2021). However, this contribution has not yet been able to surpass the effect of temperature under non-vacuum conditions. This phenomenon indicates that the effect of low partial vacuum in this study still acts as a supporting factor, while thermal energy retention plays a greater role in determining cumulative evaporation mass.

When expressed as evaporation rate per unit area, the non-vacuum condition yielded the highest value of 0.0926 kg/m²·h, followed by vacuum 2 at 0.0815 kg/m²·h and vacuum 1 at 0.0630 kg/m²·h. The evaporation mass under non-vacuum conditions was recorded to be 13.64% higher than under vacuum 2 and 47.06% higher than under vacuum 1. These results indicate that the cumulative evaporation performance was more strongly governed by the heat stored in the basin than by the relatively small pressure reduction produced by the exhaust system.

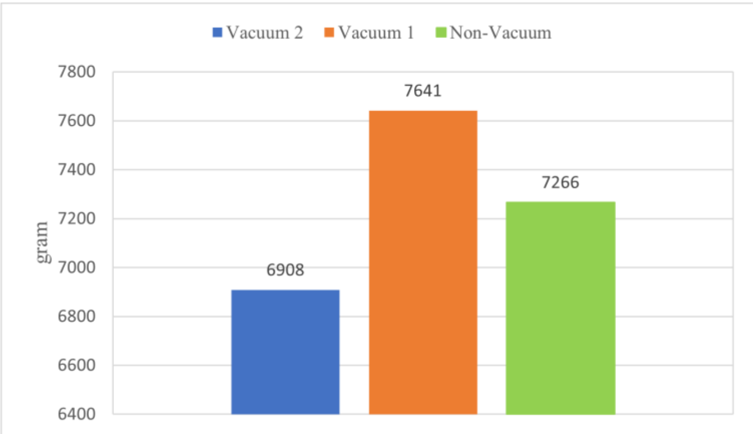

Figure 10. Condensation yield

Figure 10 shows that the highest condensation yield was obtained at vacuum level 1 (101313 Pa), amounting to 7641 grams, even though this condition did not result in the highest evaporation rate or cumulative evaporation mass. These results indicate that condensation performance is not only influenced by the amount of vapor formed during the evaporation process but is also significantly affected by the vapor distribution, the residence time of the vapor within the chamber, and the effectiveness of heat transfer during the condensation process.

Under vacuum condition 1, the decrease in partial pressure caused by a single exhaust is believed to create a more balanced condition between vapor formation and vapor distribution within the evaporation chamber. These conditions allow water vapor to have sufficient residence time before reaching the condensation surface, so that the phase change process from vapor to liquid can proceed more optimally (Munawar *et al.*, 2022). Consequently, the amount of condensate water successfully collected is higher compared to other variations. It should be noted that the exhaust fan in this study not only serves to reduce the pressure inside the evaporation chamber but also generates an airflow directed out of the solar still system.

In vacuum variation 2, the higher airflow rate caused some of the water vapor to potentially be carried out before undergoing complete condensation (Pratama, Mugisidi and Heriyani, 2026). This condition may explain why an increase in vapor pressure difference does not always result in high condensate yield, even though the driving force for evaporation increases (Curto, Franzitta and Guercio, 2021).

Under non-vacuum conditions, although the highest cumulative evaporation mass is achieved due to higher temperatures, the distribution of vapor within the chamber tends to be suboptimal. The absence of airflow to aid circulation causes some of the vapor to accumulate within the chamber, resulting in slower transport to the condensation surface (Yusuf *et al.*, 2023). Consequently, not all the vapor formed can condense effectively during the testing period. Condensation productivity per unit area showed a different trend compared to evaporation mass. Vacuum 1 produced the highest condensation productivity of 0.0809 kg/m²·h, while the non-vacuum and Vacuum 2 conditions yielded 0.0769 kg/m²·h and 0.0731 kg/m²·h, respectively. Compared to the non-vacuum condition, condensation productivity under Vacuum 1 increased by 5.16%, while compared to Vacuum 2, it increased by 10.61%.

A comparison between the mass of evaporation and the mass of condensate shows that not all the water vapor formed is successfully condensed and collected as fresh water. Under non-vacuum conditions, an average evaporation mass of 8750 g produces 7266 g of condensate, whereas under a vacuum of 2, an evaporation mass of 7700 g produces 6908 g of condensate. The difference between the mass of evaporation and the mass of condensate indicates that some vapor remains within the system chamber, adhering to the surface of the cover, or is potentially carried out along with the airflow generated by the exhaust.

This phenomenon also explains why vacuum 2 produces the highest vapor pressure difference but does not yield the highest amount of condensate. The use of two exhausts in vacuum 2 produces a greater airflow, thereby accelerating the transfer of vapor from the water surface. However, a higher airflow can also shorten the residence time of the vapor within the system chamber and increase the likelihood that some vapor will exit before undergoing complete condensation. Conversely, vacuum 1 creates a more balanced condition between vapor formation, vapor distribution, and the condensation process, thereby producing the highest amount of condensate.

In addition to evaporation mass and condensation mass, system performance was also evaluated using thermal efficiency. This parameter is used to indicate the solar still system's ability to convert the received solar radiation energy into latent energy stored in the condensed water. The higher the thermal efficiency value, the greater the fraction of solar energy successfully utilized to produce freshwater. Thermal efficiency is calculated using Equation (8) (Ismail *et al.*, 2023).

$$\eta = \frac{m_{cond} h_{fg}}{IAt} \times 100\% \quad (8)$$

where η is the thermal efficiency (%), m_{cond} is the mass of the condensate (kg), h_{fg} is the average latent heat of vaporization (J/kg), I is the average solar radiation intensity (W/m²), A is the surface area (m²), and t is the test duration (s).

An evaluation of thermal efficiency shows that vacuum 1 produced the highest efficiency of 16.17%, followed by the non-vacuum condition at 15.37% and vacuum 2 at 14.62%. Although the non-vacuum condition produced the highest evaporation mass, not all the vapor received by the system was successfully converted into condensate. Conversely, vacuum 1 was able to effectively utilize the thermal energy of the vapor to produce condensate.

Table 3. Comparison of Solar Still Performance under different operating conditions

Parameter	Variations		
	Non-Vacuum	Vacuum 1	Vacuum 2
Cumulative Evaporation Mass (g)	8750	5950	7700
Evaporation Rate (kg/m²·h)	0.0926	0.0630	0.0815
Condensation Yield (g)	7266	7641	6908
Condensation Productivity (kg/m²·h)	0.0769	0.0809	0.0731
Thermal Efficiency (%)	15.37	16.17	14.62

Based on Table 3 the results indicate that the optimal performance of a solar still system is not always determined by the rate of evaporation, but also by the balance between vapor generation, vapor distribution, and the efficiency of the condensation process within the system. These findings suggest that the use of a simple exhaust-based partial vacuum has the potential to improve the performance of the solar still system; however, the applied vacuum level must be adjusted to prevent a decrease in condensation efficiency due to changes in the vapor flow pattern within the chamber.

4. CONCLUSION

The results of the study indicate that the use of low partial vacuum increases the vapor pressure difference, thereby enhancing the driving force of evaporation during the initial stage of the test. The highest vapor pressure difference was obtained at vacuum level 2, at 1278.48 Pa. However, the highest cumulative evaporation mass was obtained under non-vacuum conditions, at 8750 g, due to the higher water temperature serving as the primary energy source for evaporation. Meanwhile, the highest condensation yield was obtained at vacuum level 1, amounting to 7641 g, with the highest thermal efficiency of 16.17%, indicating a better balance between vapor formation, vapor distribution, and the condensation process within the system. These findings suggest that increasing the vacuum level does not always result in higher freshwater production. Therefore, the optimization of a partial vacuum solar still system requires consideration of exhaust flow rate control, improved thermal insulation, condenser design development, and optimization of airflow patterns to achieve a better balance between evaporation and condensation.

ACKNOWLEDGMENTS

The authors would like to express their sincere gratitude to the salt pond research team at the Faculty of Industrial Technology and Informatics, Universitas Muhammadiyah Prof. Dr. HAMKA, for their technical support, guidance, and research funding assistance through the DPPM KEMENDIKTISAINTEK (Direktorat Penelitian dan Pengabdian kepada Masyarakat). Contract Numbers 124/C3/DT/05.00/PL/2025; 0992/LL3/AL.04/2025; 299/F03.07/2025. This support significantly contributed to the successful completion of the research and the achievement of the obtained results.

REFERENCES

Agustina, D.N.U., Sudarti and Yushardi (2020) 'Analisis Potensi Pengembangan Teknologi Desalinasi Air Laut Sebagai Penyedia Air Bersih di Desa Watukarung Kabupaten Pacitan', *Jurnal PHI : Jurnal Pendidikan Fisika dan Fisika Terapan*, 6(2), pp. 7–14. Available at: https://doi.org/10.22373/p-jpft.v6i2.9531.

Alamsyach, R. *et al.* (2024) 'Laju Penguapan Pada Forced Flow Solar Still', *Jurnal Mesin Nusantara*, 7(2), pp. 255–268. Available at: https://doi.org/10.29407/jmn.v7i2.22887.

Al-Obaidi, M.A. *et al.* (2025) 'A Review of Vacuum-Enhanced Solar Stills for Improved Desalination Performance', *Sustainability*, 17(21), p. 9535. Available at: https://doi.org/10.3390/su17219535.

Ambarita, H. (2018) 'Study of Evaporation Numerical in Seawater Desalination Evaporator using Natural Vacuum Systems', *Talenta Conference Series: Energy and Engineering (EE)*. *Seminar Ilmiah Nasional Dies Natalis USU-64*, Sumatera Utara, Indonesia: Talenta, pp. 095–103. Available at: https://doi.org/10.32734/ee.v1i1.117.

Andrés-Mañas, J.A. *et al.* (2020) 'Application of Solar Energy to Seawater Desalination in a Pilot System Based on Vacuum Multi-Effect Membrane Distillation', *Applied Energy*, 258, p. 114068. Available at: https://doi.org/10.1016/j.apenergy.2019.114068.

Ayoobi, A. and Ramezanizadeh, M. (2022) 'A Detailed Review Investigating the Mathematical Modeling of Solar Stills', *Frontiers in Energy Research*, 10, pp. 1–18. Available at: https://doi.org/10.3389/fenrg.2022.879591.

Curto, D., Franzitta, V. and Guercio, A. (2021) 'A Review of the Water Desalination Technologies', *Applied Sciences*, 11(2), pp. 1–36. Available at: https://doi.org/10.3390/app11020670.

Dina, S.F. *et al.* (2017) 'Pengaruh Tekanan Vakum Pada Proses Desalinasi Air Laut Menggunakan Tenaga Surya Tipe Kolektor Tabung Vakum', *Jurnal Teknik dan Teknologi*, 12(24), pp. 16–20.

Dwibowo, D.A. *et al.* (2025) 'Effect of Water Pressure and Temperature on The Perform-Ance of a Desalination Reactor', *Jurnal Polimesin*, 23(6), pp. 837–846. Available at: https://doi.org/10.30811/jpl.v23i6.7867.

Elazab, M.A., Elshaarawy, M.K. and Dahab, H.A. (2026) 'Optimization of Aspect Ratio for Enhanced Thermal and Exergy Efficiency in Conical Solar Distillers: A Thermodynamic And AI-Driven Study for Sustainable Freshwater Production', *Journal of Thermal Analysis and Calorimetry*, 151(7), pp. 6079–6101. Available at: https://doi.org/10.1007/s10973-026-15372-z.

Feria-Díaz, J.J. *et al.* (2022) 'Performance Evaluation of Solar Still in Veracruz, Mexico Gulf Coastline', *Water*, 14(10), pp. 1–20. Available at: https://doi.org/10.3390/w14101567.

Gaur, M.K. *et al.* (2021) 'Heat Transfer Analysis of Hybrid Active Solar Still with Water Flowing Over Glass Cover', *Journal of Thermal Engineering*, 7(6), pp. 1329–1343. Available at: https://doi.org/10.18186/thermal.989993.

Gkountas, A. *et al.* (2022) 'Modelling and Parametric Analysis of a Brine Treatment Unit Using a High-Temperature Heat Pump and a Vacuum Evaporator', *Applied Sciences*, 12(9), p. 4542. Available at: https://doi.org/10.3390/app12094542.

Haji, A.T.S., Wirosoedarmo, R. and Tyas, M.W. (2018) 'Analisis Nomografi Suhu, Laju Penguapan dan Tekanan Udara untuk Perancangan Alat Desalinasi Tenaga Surya Dengan Pengaturan Vakum', *Jurnal Sumberdaya Alam dan Lingkungan*, 4(2), pp. 1–6. Available at: https://doi.org/10.21776/ub.jsal.2017.004.02.1.

Ismail, N.R. *et al.* (2023) 'Pemanfaatan Dinding Sebagai Permukaan Kondensasi Untuk Meningkatkan Kinerja Solar Still Double Slope', *TURBO: Jurnal Program Studi Teknik Mesin*, 12(1). Available at: https://doi.org/10.24127/trb.v12i1.2439.

Lubis, A.M. and Munawar, M. (2019) 'Desalinasi Air Payau Dengan Teknik Evaporasi Surya dan Biomassa', *Prosiding Seminar Nasional Politeknik Negeri Lhokseumawe*. *Proceeding Seminar Nasional Politeknik Negeri Lhokseumawe*, Lhokseumawe, Indonesia: Politeknik Negeri Lhokseumawe, pp. A117–A120. Available at: https://e-jurnal.pnl.ac.id/semnaspnl/article/view/1674.

Mugisidi, D. *et al.* (2021) 'Determination of The Convective Heat Transfer Constant (C and N) in a Solar Still', *Jurnal Teknosains*, 11(1), pp. 1–12. Available at: https://doi.org/10.22146/teknosains.50908.

Mugisidi, D. *et al.* (2023) 'Solar Still with an Integrated Conical Condenser', *CFD letters*, 15(8), pp. 122–134. Available at: https://doi.org/10.37934/cfdl.15.8.122134.

Munawar, M. *et al.* (2022) 'Produksi Kondensat pada Sistem Desalinasi Air Asin Berbasis Energi Surya', *Prosiding Seminar Nasional Politeknik Negeri Lhokseumawe*, 6(1), pp. 44–48.

Oktavian, A. *et al.* (2024) 'Convective Coefficient and Evaporative in Forced Flow Solar Still', *Jurnal Asiimetrik: Jurnal Ilmiah Rekayasa Dan Inovasi*, 6(2), pp. 351–360. Available at: https://doi.org/10.35814/asiimetrik.v6i2.6937.

Pratama, A.C.P., Mugisidi, D. and Heriyani, O. (2026) 'Seawater Evaporation Using Natural Flow Solar Still', *TEKNOSAINS : Jurnal Sains, Teknologi dan Informatika*, 13(1), pp. 137–143. Available at: https://doi.org/10.37373/tekno.v13i1.1664.

Sachidananda, H.K. *et al.* (2025) 'Impact of Rotating Fan and Ultrasonic Humidifier on The Thermal Performance of Pyramidal Solar Still', *Scientific Reports*, 15(1), p. 38021. Available at: https://doi.org/10.1038/s41598-025-21863-0.

Sayuti, A.T. *et al.* (2023) 'The Influence of Water Temperature on Seawater Evaporation in the Desalination Process', *SINTEK JURNAL: Jurnal Ilmiah Teknik Mesin*, 17(2), pp. 113–119. Available at: https://doi.org/10.24853/sintek.17.2.113-119.

Shareef, A.S., Kurji, H.J. and Hamzah, A.H. (2024) 'Modifying Performance of Solar Still, By Using Slices Absorber Plate and New Design of Glass Cover, Experimental and Numerical Study', *Heliyon*, 10(1), pp. 1–18. Available at: https://doi.org/10.1016/j.heliyon.2024.e24021.

Susanto, S. *et al.* (2024) 'Pengaruh Perubahan Vakum dan Temperatur Pemanas Fresh Water Generator terhadap Produksi Air Tawar di MT. PM REGENT', *Saintara: Jurnal Ilmiah Ilmu-Ilmu Maritim*, 8(2), pp. 97–103. Available at: https://doi.org/10.52475/saintara.v8i2.343.

Tanusekar, H.H. and Sutanhaji, A.T. (2014) 'Rancang Bangun dan Uji Kinerja Alat Desalinasi Sistem Penyulingan menggunakan Panas Matahari dengan Pengaturan Tekanan Udara', *Jurnal Keteknikan Pertanian Tropis dan Biosistem*, 2(1), pp. 1–8. Available at: https://jkptb.ub.ac.id/index.php/jkptb/article/view/163.

Tarif, A. *et al.* (2025) 'Solar Desalination: Current Technological Status and Future Directions', *Advances in Industrial and Engineering Chemistry*, 1(1), pp. 1–17. Available at: https://doi.org/10.1007/s44405-025-00027-8.

Wirangga, R. *et al.* (2023) 'The Impact of Wind Speed on the Rate of Water Evaporation in a Desalination Chamber', *Journal of Advanced Research in Fluid Mechanics and Thermal Sciences*, 106(1), pp. 39–50. Available at: https://doi.org/10.37934/arfmts.106.1.3950.

Yan, T. *et al.* (2021) 'Experimental Study on Three-Effect Tubular Solar Still Under Vacuum and Immersion Cooling', *Desalination*, 515, p. 115211. Available at: https://doi.org/10.1016/j.desal.2021.115211.

Yusuf, A.M. *et al.* (2023) 'Effect of Vacuum on Evaporation of Seawater: Pengaruh Vakum Pada Penguapan Air Laut', *R.E.M. (Rekayasa Energi Manufaktur) Jurnal*, 8(2), pp. 55–62. Available at: https://doi.org/10.21070/r.e.m.v8i2.1672.